PCCP

The effect of flexibility on the phase diagram of simple molecular models

Carlos Vega,* Carl McBride and Luis G. MacDowell

Departamento de Química Física, Facultad de Ciencias Químicas, Universidad Complutense de Madrid, Ciudad Universitaria, 28040, Madrid, Spain. E-mail: carlos@ender.quim.ucm.es

Received 3rd September 2001, Accepted 5th November 2001
First published as an Advance Article on the web 8th January 2002

In this paper the effect of molecular flexibility on the phase diagram is studied. Three groups of models are used; a pearl-necklace model, a linear tangent hard sphere model and a hybrid model consisting of a rigid section and a flexible section. Each of these models are built up from hard sphere interaction sites. Calculations of the virial coefficients show significant differences between each of the models. In spite of this the equation of state is hardly affected by flexibility in the medium density range. However, at higher densities flexible and linear rigid chains display significant differences; the former having only fluid and solid phases whereas the the rigid model also forms mesophases (nematic and smectic A). The introduction of flexibility into a rigid model has the effect of moving the onset of liquid crystal formation to higher densities. Flexibility is also seen to stabilize the smectic phase at the expense of the nematic phase. Critical properties have been obtained from Wertheim's thermodynamic perturbation theory (TPT1) in the limit of infinitely long chains. Zero number density of chains, zero mass density and pressure and finite non-zero values of the critical temperature and compressibility factor are predicted at the critical point. For very long chains the critical temperature (*i.e.* the Θ temperature) is seen to be the Boyle temperature. From Wertheim's theory it is possible to analytically determine the temperature Θ for square well chains.

I. Introduction

Molecular fluids may be classified in a number of ways.[1] One such classification is by molecular shape; simple fluids (usually spherical particles) are often used to represent the noble gases, or linear and angular fluids which can be used to represent diatomic molecules and triatomic molecules (*i.e.* CO_2). Another possibility is to consider the presence or absence of multipolar moments, for example classifications such as non-polar, quadrupolar, dipolar, ionic *etc*. Molecular fluids can also be classified depending on whether flexibility is present or absent in the model. It is important to clarify the meaning of molecular flexibility in this context: clearly no real molecule is completely rigid. All molecules suffer constant structural changes in the way of fluctuations. However, in very few cases do these fluctuations assume magnitudes greater than 1% of its equilibrium value. In view of this to a first approximation it is reasonable to assume that these molecules are 'rigid'. For rigid molecules it is possible to obtain good estimates of configurational properties by fixing the molecular geometry to the molecular equilibrium values. However, for organic molecules, for example butane,[2] their thermal energy at room temperature is sufficient to overcome internal energy barriers, leading to conformational changes. Molecules that have ready access to a number of conformations are clearly flexible. In the calculation of configurational properties the existence of flexibility should be considered from the very outset. Hybrid molecules fall between the cases of rigid molecules at one extreme, and flexible molecules, such as polymers and alkanes, at the other. A hybrid molecule would be one for which certain sections are rigid, and other sections have a high degree of flexibility. A large number of mesogenic molecules (those forming liquid crystal phases) belong to this class. A common example of such a mesogenic molecule is 4-pentyl-4′-cyanobiphenyl,[3,4] having a rigid section composed of a pair of benzene rings, and a flexible alkyl tail.

The focus of this paper is on the phase diagrams and equation of state (EOS) for completely flexible molecules, hybrid molecules, and completely rigid molecules. The primary motivation for this work is the identification of the role of molecular flexibility on the phase diagram. In order to isolate the effect of flexibility on the phase diagram molecular features that could make the comparison of rigid and the flexible models ambiguous have not been incorporated, for example electrostatic charges are not included in this study. The molecular models used in this study are built up from m hard sphere monomers.[5] Three models have been used in this study. The first model is the so called 'pearl-necklace' model.[6–8] This model consists of hard sphere monomers which are tangentially bounded and are free to adopt any non-overlapping configuration (see Fig. 1). The pearl-necklace model represents a completely flexible molecule. On the other hand a completely rigid molecule has been studied using the linear tangent hard sphere model (LTHS) also shown in Fig. 1. Advantages of using a hard sphere potential are that the EOS and phase diagram no longer depend on temperature but rather on the

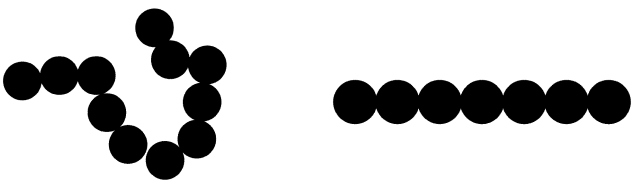

Fig. 1 The pearl-necklace model (left) and the LTHS model (right)

DOI: 10.1039/b107988n

This journal is © The Owner Societies 2002

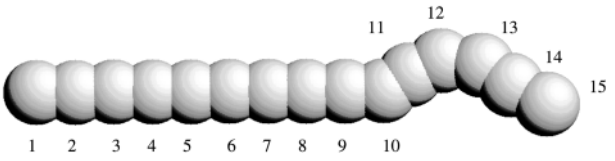

Fig. 2 The hybrid (RFFFHS) model for $m_r = 10$ and $m_f = 5$

density of the system. Another advantage is that the absence of attractive forces removes the vapor–liquid equilibria region from the phase diagram, thus making any analysis easier. As well as the pearl-necklace model and the LTHS model a hybrid model has been studied.[9] The hybrid, or rigid fully flexible fused hard sphere (RFFFHS) model, consists of a rigid section formed from m_r hard spheres and a flexible part having m_f hard spheres (see Fig. 2). In the hybrid model the monomer units are no longer tangential, but rather overlapping, with a reduced bond length of 0.6. The overlap of the monomer units makes the model more 'convex' than the tangent hard sphere case, which is an advantage in the study of high density fluids, such as liquid crystals. This reduced bond length also allows flexibility to be introduced more gradually than in the tangent case.

In order to study the vapor–liquid equilibria attractive forces must be present. In view of this we present results for flexible chains composed of Lennard-Jones monomers, with special emphasis given to the critical properties of very long chains.

It is important that simulation results should be viewed alongside theoretical results. In the early nineteen eighties Wertheim proposed a theory for associating fluids.[10–14] When the association between sites becomes infinitely strong, chain-like fluids are formed. Starting with the EOS and structural properties of the reference system formed by non-associating monomers, the EOS and free energy of the chain fluid formed by tangent monomers can be obtained by using a perturbative approach. Wertheim's theory, when truncated at the first order, is known as the first order perturbation theory (TPT1).[15] One of the most striking conclusions of TPT1 is the prediction that the EOS does not depend on chemical details such as bond angles or the presence or absence of flexibility. This surprising result has been tested for short chains and it has indeed been found that flexibility has very little effect on the isotropic EOS.[16] However one may suspect that this finding can not hold true for long chains; fully flexible chains do not form liquid crystal phases whereas fully rigid chains do indeed form mesophases. In this work we shall make a detailed comparison of the behavior of rigid and flexible hard chains, from the very low density region up to the high density and solid phase, and analyse the differences between rigid and flexible chains.

The scheme of the paper is as follows. In Section II we outline Wertheim's first order perturbation theory (TPT1). In Section III a detailed comparison between the LTHS model and the pearl-necklace model will be provided for the low density region III.A, in the medium density region III.B and in the high density region III.C. In Section IV we present results for a model containing rigid and flexible units. In Section V we shall briefly describe some results concerning the vapor–liquid equilibrium of flexible chains. Finally in Section VI the conclusions are presented.

II. Brief description of Wertheim's perturbation theory

We shall summarize the main ideas contained within Wertheim's theory by following the thermodynamic cycle introduced by Zhou and Stell.[17] We have a reference fluid containing a number of spherical particles or monomers N^{ref} within a volume V at a temperature T. These particles interact through a spherical pair potential $u(r)$. The properties of this reference fluid will be labeled by the superscript ref. In a second container of volume V and temperature T, there are $N = N^{ref}/m$ fully flexible chains of m monomers each. By fully flexible chains we mean chains of m monomers, with a fixed bond length of $L = \sigma$, and no other constraints (*i.e.* there are no bond angle potentials or torsional terms). Each and every monomer interacts with all other monomers in the system, regardless as to whether they are in the same molecule or not. Residual properties of the reference fluid are described by the properties of the reference fluid minus those of an ideal gas at the same number density and temperature. Residual properties of the chain fluid are defined as those of the chain fluid minus those of an ideal gas of chains at the same number density (of chains) and temperature. Notice that in the ideal gas of chains there are no intermolecular interactions but intramolecular interactions are still present.

The thermodynamic cycle of Zhou and Stell is presented in Fig. 3. In the upper left section is an ideal gas of monomers. In the upper right section is an ideal gas of chains. In the lower left section is the reference fluid with monomers interacting *via* the pair potential $u(r)$ and in the lower right section the chain fluid where inter- and intra-molecular interactions are also described by $u(r)$. Because we have a thermodynamic cycle it holds that

$$\Delta A_{step4} = \Delta A_{step1} + \Delta A_{step2} + \Delta A_{step3} \quad (1)$$

The meaning of ΔA_{step1} and ΔA_{step3} is clear since they are related to the residual properties of the reference fluid and of the chain fluid:

$$\Delta A_{step1} = -A^{ref}_{residual} \quad (2)$$

$$\Delta A_{step3} = A_{residual}. \quad (3)$$

The change in free energy for step 2 is given by:

$$\Delta A_{step2} = -NkT\ln(\exp(-\beta U_{intra,chain})) \quad (4)$$

The change of free energy in step 4 is unknown. Two approximations shall now be made. We shall assume that the work done in forming N chains is identical to N times the work done to form the first chain in the monomer reference fluid, thus:

$$\Delta A_{step4} \approx -NkT\ln(g^{ref}(\boldsymbol{r}_1, \boldsymbol{r}_2, \ldots, \boldsymbol{r}_m)) \quad (5)$$

where g^{ref} $(\boldsymbol{r}_1, \boldsymbol{r}_2, ..., \boldsymbol{r}_m)$ is the m-body correlation function of

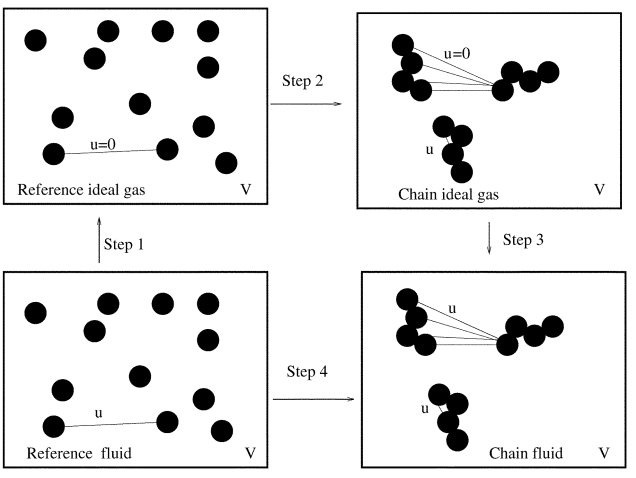

Fig. 3 Thermodynamic cycle representing Wertheim's theory.

the reference fluid. Introducing this approximation into eqn. (1) one obtains:

$$A_{\text{residual}} = A^{\text{ref}}_{\text{residual}} - NkT\ln(y^{\text{ref}}(\boldsymbol{r}_1, \boldsymbol{r}_2, \ldots, \boldsymbol{r}_m)) \qquad (6)$$

where y^{ref} ($\boldsymbol{r}_1$, $\boldsymbol{r}_2$,...,$\boldsymbol{r}_m$) is the background correlation function of the reference fluid. This function is in general unknown. A second approximation is needed. The m-body background correlation function of the reference fluid will be approximated by:

$$y(\boldsymbol{r}_1, \boldsymbol{r}_2, \ldots, \boldsymbol{r}_m) = y^{\text{ref}}(r_{12})y^{\text{ref}}(r_{23}) \cdots y^{\text{ref}}(r_{m-1,m}) \qquad (7)$$

Therefore the residual free energy of the chain fluid is given by:

$$A_{\text{residual}} = A^{\text{ref}}_{\text{residual}} - N(m-1)kT\ln(y^{\text{ref}}(\sigma)) \qquad (8)$$

and the total free energy of the chain is given by:

$$\frac{A}{NkT} = \ln(\rho\sigma^3) - 1 + \frac{A^{\text{ref}}_{\text{residual}}}{NkT} - (m-1)\ln(y^{\text{ref}}(\sigma)) \qquad (9)$$

where ρ is the number density of chains, given by

$$\rho = \frac{N}{V} \qquad (10)$$

and the EOS of the chain fluid is given by:

$$Z = \frac{p}{\rho kT} = mZ^{\text{ref}} - (m-1)\left(1 + \rho^{\text{ref}}\frac{\partial\ln(y^{\text{ref}}(\sigma))}{\partial\rho^{\text{ref}}}\right) \qquad (11)$$

where ρ^{ref} is the number density of monomers, Z is the compressibility factor of chains, and Z^{ref} is the compressibility factor of the reference fluid. Eqns. (9) and (11) constitute the basic equations of Wertheim's TPT1 theory. So far we have placed no restraint on the nature of the pair potential $u(r)$. The previous two equations can be applied equally well to chains formed by hard spheres of diameter σ, or to Lennard-Jones (LJ) chains with distance between contiguous monomers equal to σ. In both cases the background correlation at contact $y^{\text{ref}}(\sigma)$, is identical to the pair correlation function at contact $g^{\text{ref}}(\sigma)$ (*i.e.* $u(\sigma)=0$). According to TPT1, in order to obtain the thermodynamic properties of the chain fluid, one must first know the thermodynamic properties of the reference fluid, and their structural properties as given by $g^{\text{ref}}(\sigma)$. Wertheim's TPT1 has already been implemented for hard sphere chains, for LJ chains in the fluid phase,[18,19] and for chains consisting of non-spherical segments.[20] However, notice that the previous equations can also be applied to the solid phase; all that is required is a knowledge of the thermodynamic and structural properties of the reference fluid for the solid. As will be shown later eqns. (9) and (11) constitute a good description of the thermodynamic properties of chains in the solid phase. In summary:

(i) Wertheim theory provides the EOS and free energy of chains, as long as the free energy and the structure of the reference system of monomers is known.

(ii) The reference monomers can be in the fluid or in the solid phase, with either a hard sphere or a LJ pair potential.

(iii) No distinction is made in Wertheim's theory between rigid and flexible chains.

Notice that in both of the models the bonds are distributed isotropically in the fluid and in the solid phase (as will be discussed later fully flexible chains form solid phases with a random distribution of bond vectors). However, one may suspect that Wertheim's theory (at least its first order implementation) can not be successful in describing phases where the bonds between monomers are oriented, as it is the case of the LTHS model in the nematic, smectic, or solid phase.

The implementation of Wertheim's TPT1 for the system of fully flexible tangent hard spheres in the fluid phase (when used in conjunction with the Carnahan–Starling EOS[21] for the monomer fluid) is particularly simple and yields:

$$Z = \frac{p}{\rho kT} = m\frac{1 + y + y^2 - y^3}{(1-y)^3} - (m-1)\frac{1 + y - y^2/2}{(1-y)(1-y/2)} \qquad (12)$$

where V_{m} is the molecular volume given as $V_{\text{m}} = \frac{\pi m}{6}\sigma^3$, and y is the volume fraction given by $y = \rho V_{\text{m}}$. Alternative equations of state that satisfactorily describe the EOS of the pearl-necklace model are the generalized Flory-dimer theory,[6] the perturbed hard sphere chain[22] and the integral approach of Chiew.[23]

III. Results

A The very low density region

At sufficiently low densities the EOS of a fluid can be described by the virial expansion. The pressure of a homogeneous isotropic fluid can be given in terms of a power series of the density by the following expression:

$$Z = \frac{p}{\rho kT} = 1 + B_2(T)\rho + B_3(T)\rho^2 + B_4(T)\rho^3 + \ldots \qquad (13)$$

where B_2, B_3 and B_4 are the second, third and fourth virial coefficients, respectively. For a hard body system the virial coefficients do not depend on T hence eqn. (13) can be written as

$$Z = 1 + B_2^* y + B_3^* y^2 + B_4^* y^3 + \ldots \qquad (14)$$

where B_n* are the reduced virial coefficients, defined as:

$$B_n^* = \frac{B_n}{V_m^{n-1}}. \qquad (15)$$

Although the virial coefficients of rigid molecules can be evaluated by the procedure proposed by Ree and Hoover[24] (extended to non-spherical molecules by Rigby[25,26]) the evaluation of the virial coefficients for flexible molecules is non-trivial. We have recently proposed a methodology to evaluate the virial coefficients of multicomponent mixtures. An extension of this methodology allows one to compute the virial coefficients of flexible molecules. Basically the different configurations which may be adopted by the chain are treated as different components of a mixture. Details of the procedure may be found in ref. 27 Let us first consider the case of short chains (*i.e.* $m<8$). In Tables 1 and 2 the virial coefficients of rigid and flexible chains with $m=4$, 5, 6, 7, 8 are presented. Results for the LTHS were taken from Vega *et al.*[28] whereas the results for the pearl-necklace model were obtained in this work. As can be seen, clear differences are visible between the virial coefficients of rigid and flexible chains.

Table 1 Calculated virial coefficients for the fully rigid model

m	B_2*	B_3*	B_4*
4	8.248	32.36	57.94
5	9.641	40.67	60.94
6	11.033	49.49	56.47
7	12.423	58.48	42.55

Table 2 Calculated virial coefficients for the pearl-necklace model

m	B_2*	B_3*	B_4*
5	8.483	38.25	94.03
6	9.379	45.72	115.88
7	10.117	52.76	138.69

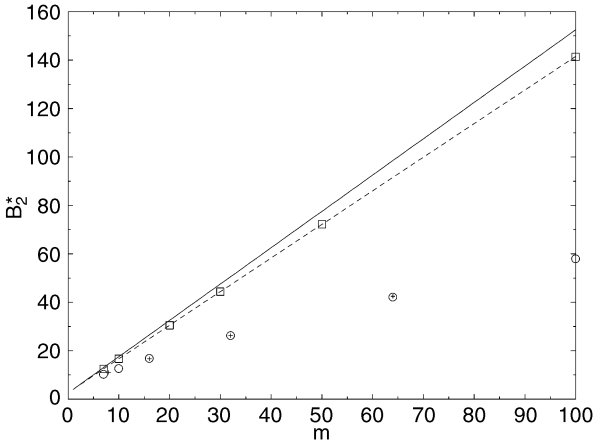

Fig. 4 Reduced second virial coefficient B_2* for hard models made up of m tangent hard spheres. Numerical results of this work for the pearl-necklace model (open circles); numerical results for the pearl-necklace model from Yethiraj *et al.*[30] (plus sign); Wertheim TPT1 predictions (solid line); numerical results of this work for the LTHS model (open squares); exact predictions[31,32] for the LTHS (dashed line).

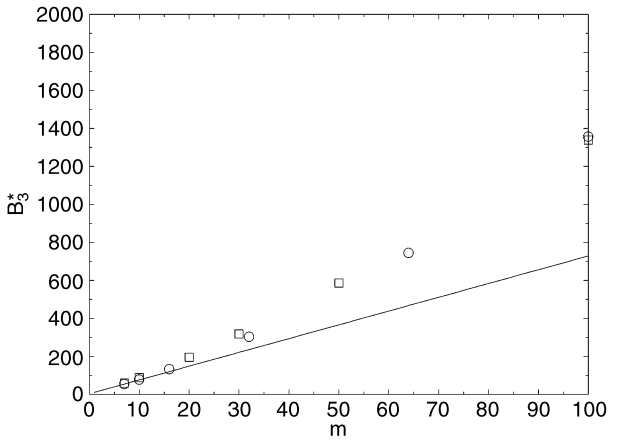

Fig. 5 Reduced third virial coefficient B_3* of models formed by m tangent hard spheres. Numerical results of this work for the pearl-necklace model (open circles); Wertheim's TPT1 predictions (solid line); numerical results of this work for the LTHS model (open squares).

The case of very long chains (with m up to 200) has also been considered.[29] In Fig. 4 and Fig. 5, the values of B_2 and B_3 for the LTHS and for the pearl-necklace model are presented along with the predictions of TPT1 for this system. We notice that differences in B_2 are significant whereas differences in B_3 are much smaller. Wertheim's hypothesis of identical EOS for flexible and rigid chains seems to be supported by our results for B_3 but not by our results for B_2. An interesting issue is the scaling law followed by the virial coefficients. For the second virial coefficient the scaling laws are well known. For flexible chains it holds that[30]

$$B_2 \propto m^{3\nu} \propto m^{1.8} \tag{16}$$

where ν is the exponent of the radius of gyration under good solvent conditions ($\nu \approx 0.6$). For rigid linear chains:[31,32]

$$B_2 \propto m^2 \tag{17}$$

However, the scaling of higher virial coefficients is not so clear. For hard flexible chains De Gennes proposed[33] (in good solvent conditions) that $B_i \propto m^{(3\nu)(i-1)}$. One consequence of this is that for flexible chains:

$$\lim_{m\to\infty} \frac{B_n}{B_2^{n-1}} = \lim_{m\to\infty} \frac{B_n^*}{\left(B_2^*\right)^{n-1}} = g_n. \tag{18}$$

For rigid linear chains, Onsager proposed[34] that:

$$\lim_{m\to\infty} \frac{B_n}{B_2^{n-1}} = \lim_{m\to\infty} \frac{B_n^*}{\left(B_2^*\right)^{n-1}} = 0. \tag{19}$$

In order to test whether our numerical results are compatible with these scaling laws, results are presented in Fig. 6 and Fig. 7 for B_3 and B_4. Our results are fully consistent with Onsager's scaling for linear rigid chains (this could be expected since hard spherocylinders present Onsager scaling and our LTHS model should follow an identical scaling[35–37]), and de Gennes' scaling for flexible chains. The g_3 factor of de Gennes scaling obtained from our results is close to 0.35 for B_3. For B_4 it is more difficult to make an assessment on the value of g_4; it seems that our results are not in the asymptotic regime.

In summary the virial coefficients of flexible and rigid chains differ significantly in both magnitude and scaling behavior for large values of m. Therefore both rigid and flexible chains show important differences in the very low density regime. One may

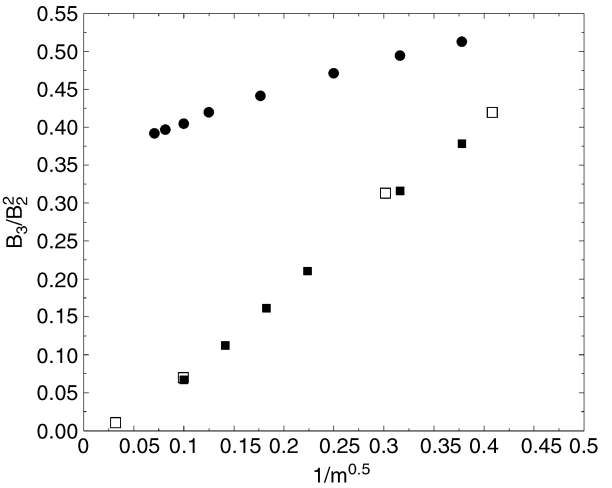

Fig. 6 B_3/B_2^2 plotted as a function of $1/\sqrt{m}$ for several hard models. Results for the pearl-necklace model obtained in this work ●, results for LTHS obtained in this work ■, and results for hard spherocylinders from ref. 35 □.

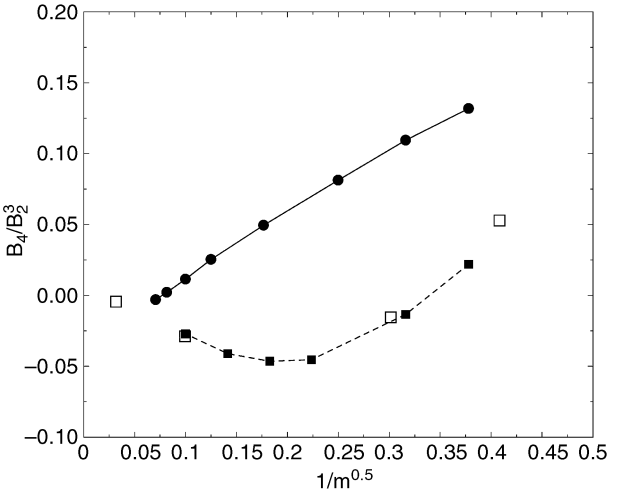

Fig. 7 B_4/B_2^3 plotted as a function of $1/\sqrt{m}$. Symbols as in Fig. 6.

suspect that the osmotic second virial coefficients of polymers under good solvent conditions are sensitive to the presence or absence of flexibility.

B The medium density region

When the virial expansion starts to break down we enter into the medium density regime. In Fig. 8 the EOS for $m = 3$, 5 and 7 for the LTHS and for the pearl-necklace model as obtained from simulation are presented as well as the predictions from Wertheim's TPT1. As can be seen, the EOS for rigid and flexible chains are similar in the medium density region. At medium densities the compressibility factors of LTHS are always lower than those of flexible chains. Wertheim's TPT1 describes quite well both sets of data, but seems to be better at reproducing the simulation results for the flexible model. Another interesting feature is the existence of a crossing in the EOS (compressibility factor *versus* volume fraction) of rigid and flexible chains which have the same value of m. In fact at very low densities the LTHS model presents a higher value of the compressibility factor for a certain value of m than the flexible chain model. This is a consequence of the scaling m^2 for B_2 of LTHS *versus* the $m^{3\nu}$ scaling of B_2 for flexible chains. However at medium densities LTHS has lower values of Z for a certain value of y than flexible chains. Therefore the EOS of rigid and flexible chains with the same value of m do indeed cross. One may suspect that this is due to the much lower value of B_4 of rigid chains than that of flexible chains. At medium densities where the contribution of B_4 is important the EOS of the LTHS is lower than that for flexible chains. It is somewhat surprising that Wertheim's TPT1 correctly predicts the EOS for these models, especially when taking into account that it fails completely in describing the virial coefficients, as was shown in Section III.A.

C The high density region

We shall now focus on the high density region. The phase diagram of the pearl-necklace model has been determined recently by Malanoski and Monson[38] from computer simulation results. The only phases found for the pearl-necklace model are the isotropic fluid phase and the solid phase. The solid phase of the pearl-necklace model is particularly interesting since it consists of a fcc close packed structure of atoms with a random distribution of bond vectors.[38,39] In Fig. 9 a two dimensional sketch of a high density phase of the pearl-necklace model is shown. In the previous section we have shown

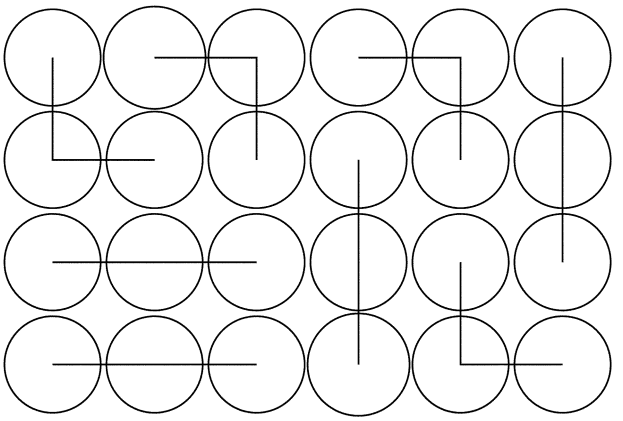

Fig. 9 Schematic diagram of the flexible trimer in the solid phase.

that TPT1 successfully describes the simulation results of the pearl-necklace model in the fluid phase. Can TPT1 be extended to describe the solid phase? In Fig. 10 the EOS as obtained from Wertheim's TPT1 for the solid phase is presented along with the simulation results of Malanoski and Monson. As can be seen the agreement between theory and simulation is quite good. The extension of Wertheim's theory to the solid phase is straightforward (details may be found in ref.40) requiring only the EOS and free energy of the hard sphere solid. The fact that Wertheim's theory can be used to describe the solid phase of the pearl-necklace model seems to have been overlooked previously. Not only is the EOS of the solid phase good, but also the free energies as well. In Fig. 11 the fluid–solid equilibrium of the pearl-necklace model as obtained from simulation and from Wertheim's TPT1 theory (for the fluid and solid phase) is presented. As can be seen the agreement between theory and simulation is again quite good. The theory is able to predict an asymptotic limit for the volume fractions of chains at freezing for large values of m. In fact the extension of Wertheim's theory to the solid phase has shown that asymptotic values of freezing properties are obtained whenever the EOS and free energies of the chains in the fluid and in the solid phases are linear functions of m. Let us now examine the LTHS model. The solid structure is based again on a close packed fcc structure of hard spheres with stacking sequence ABCABC (see Fig. 12). The molecules are constructed by linking m monomers in a linear configuration. The same orientation is assigned to each of the molecules in each of the layers. The final solid structure corresponds to the CP1 structure in the

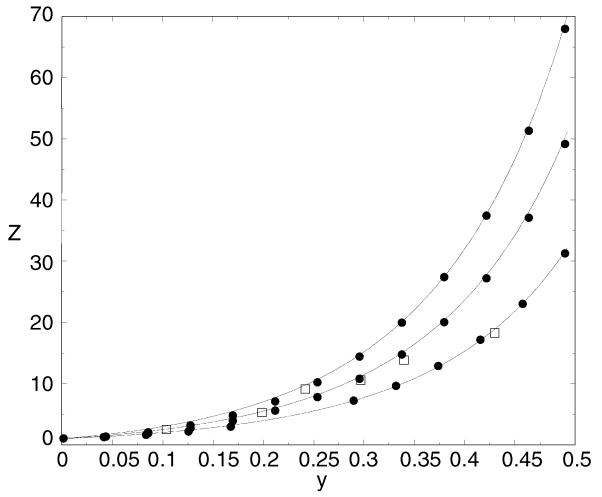

Fig. 8 From top to bottom results for $m = 7$, 5 and 3. Circles: simulation results for flexible chains. Squares: Simulation results for rigid chains. Lines: TPT1.

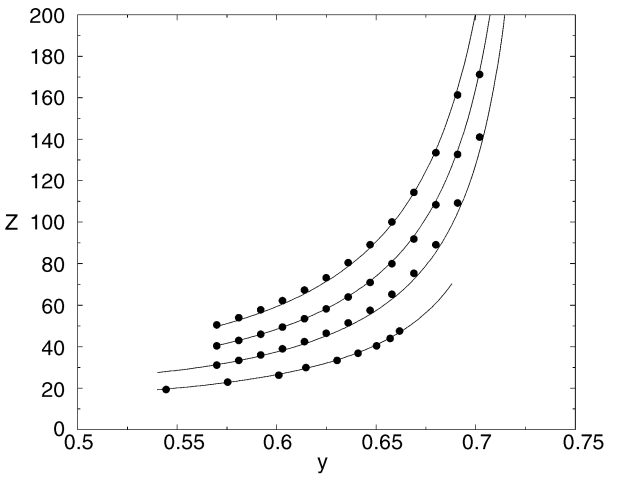

Fig. 10 Equation of state for the pearl-necklace model in the solid phase. Symbols: Simulation results. Solid line: Wertheim's theory.

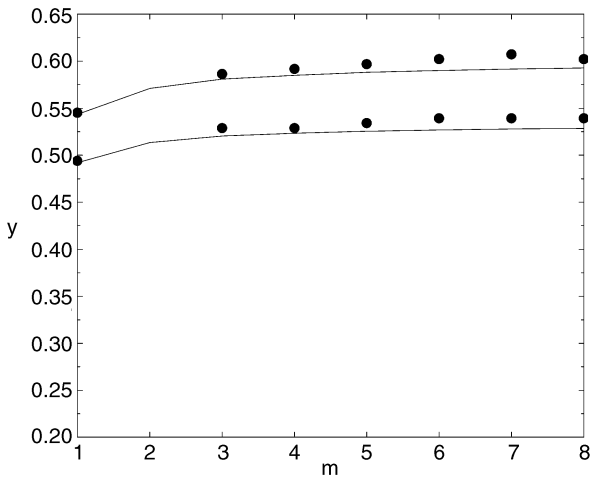

Fig. 11 Solid–fluid equilibrium of the pearl-necklace model. Symbols: Simulation results.[38] Solid line: Wertheim's theory.

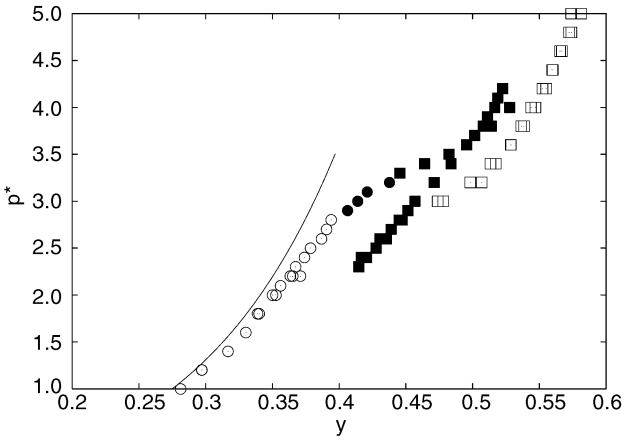

Fig. 13 Plot of the EOS for the 5 LTHS model. ○ represents isotropic state points, ● represents nematic state points, ■ represents smectic state points and □ represents solid state points. The solid curve is the TPT1 EOS. $p^* = p/(kT)\sigma^3$.

paper by Vega *et al.*[41] for the solid phases of hard dumbbells. The solid structure for the LTHS model with $m = 5$ is shown in Fig. 12. Notice that the molecular axis is tilted with respect to the layer normal (*i.e.* to the A plane of the fcc hard sphere solid). We have performed NpT Monte Carlo simulation (MC) runs. Non-isotropic Monte Carlo was used to allow for changes of shape in the simulation box.[42] Expansion runs started from a high density solid, and compression runs started from a low density gas (for details see ref. 43). For $m = 4$ no liquid crystal phase was obtained. For $m = 5$ a smectic A structure was obtained in the expansion runs. For $m = 6$, nematic and smectic A phases were found for both compression and expansion runs. The EOS as obtained from the simulation runs is presented in Fig. 13 for $m = 5$ and in Fig. 14 for $m = 6$, along with predictions from the Vega–Lago theory[44] for the isotropic–nematic transition (lines). In addition to isotropic fluid and solid phases, mesophases are obtained for the LTHS model.[43,45] For $m = 6$, nematic and smectic A phases were obtained. The behavior of the LTHS differs significantly from the pearl-necklace model. In Fig. 15 the EOS for the LTHS and for the pearl-necklace model with $m = 6$ is given. As can be seen, rigid and flexible molecules display quite similar behavior up to volume fractions of $y = 0.32$. For higher densities the EOS is completely different. This is mainly due to the fact that the LTHS model can form liquid crystal phases whereas the pearl-necklace model can not. Even in the solid phase the EOS of the two models is quite different. This is interesting since the close packing density for the two models is

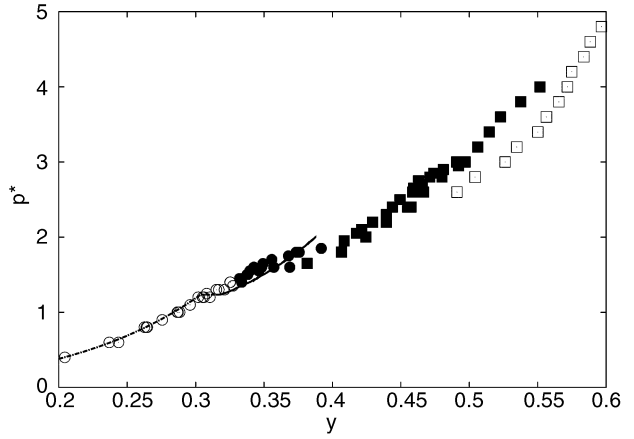

Fig. 14 Plot of the EOS for the 6 LTHS model. ○ represents isotropic state points, ● represents nematic state points, ■ represents smectic state points and □ represents solid state points. The dot-dashed curve is the Vega–Lago theory for the isotropic phase, the dashed line represents the tie line and the solid curve for the nematic phase. $p^* = p/(kT)\sigma^3$.

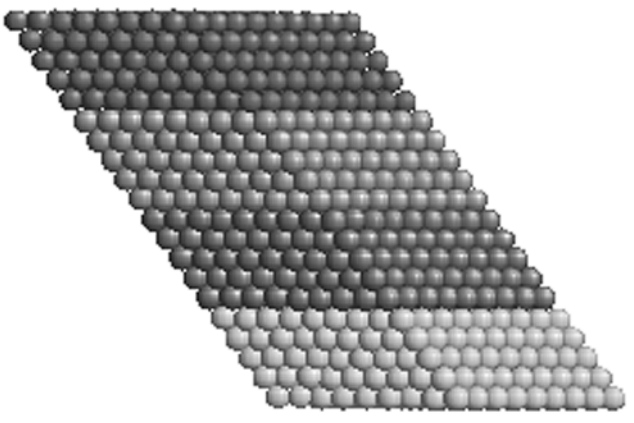

Fig. 12 Solid structure of the LTHS with $m = 5$.

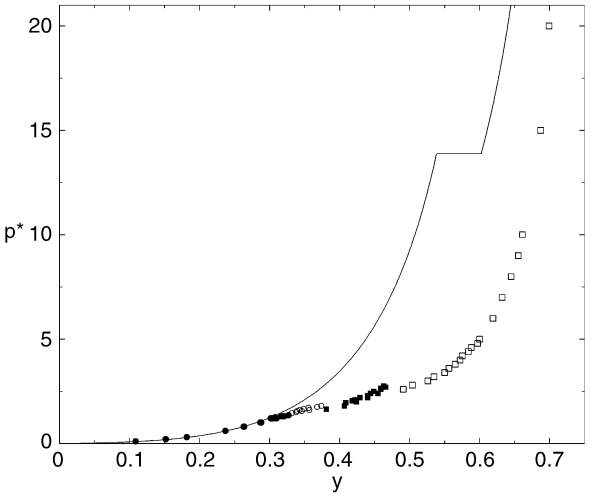

Fig. 15 EOS for the $m = 6$ model. Solid line: Flexible model, and the symbols represent the fully rigid model; ● isotropic, ○ nematic, ■ smectic, □ solid.

the same, namely that of the hard sphere system $y = \sqrt{2}\pi/6$.. The message of Fig. 15 is that rigid and flexible chains present quite different behavior. Let us briefly describe how Fig. 15 would be for large values of m (and not just for $m = 6$). It turns out (and this can be shown by our implementation of Wertheim's theory) that for the pearl-necklace model, the p^* *versus* y plot is hardly affected by m. In other words when m becomes very large the p^* *versus* y representation is practically identical to that presented in Fig. 15 for $m = 6$. The results presented in Fig. 15 are very close to this asymptotic limit. However for the LTHS the diagram changes quite dramatically with m. Basically as m increases the p^* becomes smaller for a certain value of y. The I–N transition moves to lower and lower densities as m increases and therefore the range where the N phase is stable increases. The volume fractions at which the N–SmA or SmA–solid phase transitions occur are hardly affected by the value of m. This is expected if one examines the phase diagram of hard spherocylinders obtained by Bolhuis and Frenkel.[46]

IV. Hybrid model

The hybrid model consists of 15 overlapping hard sphere interaction sites,[9] with one extreme of the model being flexible and the other extreme completely rigid. Simulations were performed using configurational bias Monte Carlo.[47] We shall classify the models by the number of monomers in the rigid section followed by the number of monomers in the flexible section. For example, the model with nine rigid monomers and six flexible monomers is the "9 + 6" model. The results for the EOS for the RFFFHS model for the models 15 + 0, 13 + 2, 11 + 4, 10 + 5, 9 + 6 and 8 + 7 are given in Fig. 16. In the isotropic region the equation of state for each of the models closely follow the TPT1 EOS. It is important to note that the TPT1 EOS was designed for non-overlapping monomers. In order to apply TPT1 to the RFFFHS model we make use of the correction of Zhou *et al.*[48] This correction provides an effective number of monomers, m_{eff} for use in TPT1. For $L^* \geqslant 0.5$ this is given by

$$m_{\text{eff}} = \frac{(1 + (m-1)L^*)^3}{(1 + (m-1)L^*(3 - L^{*2})/2)^2}. \qquad (20)$$

From Fig. 16 it can be seen that TPT1 is not only insensitive to difference between fully rigid and fully flexible models, but also for a hybrid model which is part rigid and part flexible. Results

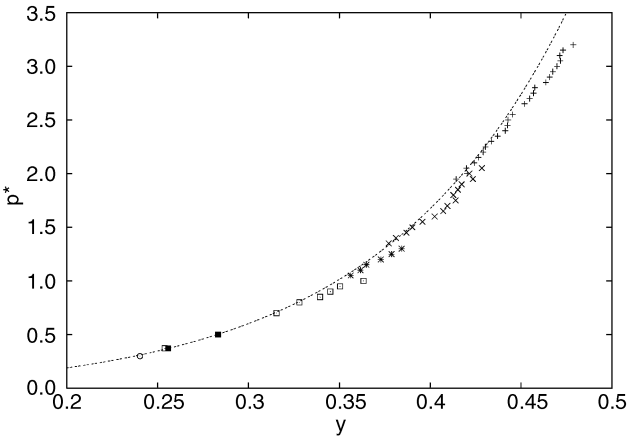

Fig. 16 Monte Carlo results for the EOS of the RFFFHS models in the isotropic phase at medium densities (symbols). Results correspond to (+) 8 + 7, (×) 9 + 6, (*) 10 + 5, (□) 11 + 4, (■) 13 + 2 and (○) 15 + 0. The dashed line represents the TPT1 EOS using the Zhou *et al.* implementation.[48]

Table 3 Calculated virial coefficients for the isotropic phase

m_r	m_f	B_2^*	B_3^*	B_4^*
15	0	12.906 ± 0.002	55.86 ± 0.03	− 9.1 ± 0.26
14	1	12.854 ± 0.003	56.16 ± 0.03	− 2.8 ± 0.21
13	2	12.737 ± 0.008	56.50 ± 0.02	5.5 ± 0.14
12	3	12.602 ± 0.006	56.81 ± 0.08	14.6 ± 0.31
11	4	12.469 ± 0.015	57.21 ± 0.03	23.3 ± 0.86
10	5	12.239 ± 0.008	57.51 ± 0.14	23.3 ± 0.86
9	6	12.115 ± 0.019	57.95 ± 0.12	46.1 ± 0.91
8	7	11.879 ± 0.003	58.20 ± 0.13	60.5 ± 1.02

for the virial coefficients in the isotropic phase are given in Table 3.

As the packing fraction is increased liquid crystalline phase formation is observed. In the 15 + 0 model nematic and smectic phases are observed. Similarly for the 13 + 2, the 11 + 4 and the 10 + 5 models. However, a decrease in the nematic region is found and the smectic region grows. This indicates that the flexible tails help to stabilize the smectic phase and reduce the nematic range. It is debatable as to whether there exists a nematic range for the 9 + 6 model, and the 8 + 7 shows no signs of liquid crystal phase formation. The simulation results are summarized in Fig. 17.

V. Soft potential

In this section we focus on flexible Lennard-Jones (LJ) chains. In the flexible LJ model each of the monomer sites is the center for a LJ potential.[5] Due to the presence of attractive forces the model now presents a vapor–liquid equilibria region. Little is known about the global phase diagram of this model (vapor, liquid, and solid regions). Previous work has mainly focused on the vapor–liquid equilibria, obtained either by way of computer simulation or by theory.[49–51] Here we focus on the vapor–liquid equilibria of this model in the limit of very large values of m. As mentioned in Section II, Wertheim's TPT1 can be used to describe LJ chains. The only requirement is a knowledge of the EOS and structural properties (*i.e.* $g_{\text{ref}}(\sigma)$) of the reference LJ fluid. In particular we shall analyse the predictions of Wertheim's TPT1 concerning the scaling of the critical properties in the limit of large values of m.

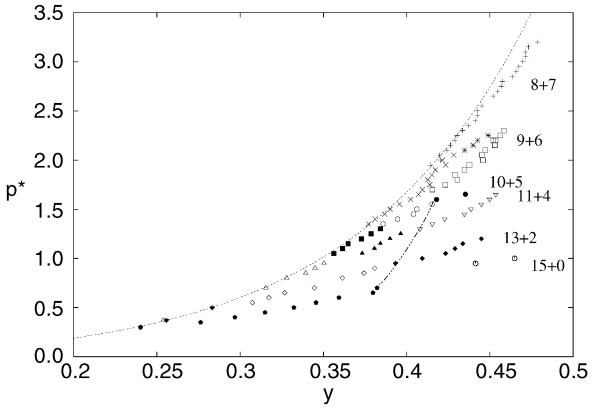

Fig. 17 The equation of state from the MC simulations. (+) 8 + 7 (isotropic); (×) 9 + 6 (isotropic); (*) 9 + 6 (nematic); (□) 9 + 6 (smectic); (■) 10 + 5 (isotropic); (⊙) 10 + 5 (nematic); (●) 10 + 5 (smectic); (△) 11 + 4 (isotropic); (▲) 11 + 4 (nematic); (∇) 11 + 4 (smectic); (▼) 13 + 2 (isotropic); (◇) 13 + 2 (nematic); (◆) 13 + 2 (smectic); solid black pentagon 15 + 0 (nematic), and the 15 + 0 (smectic) is a bold open circle. The dotted curve represents the TPT1 EOS for the 15 + 0 RFFFHS model using the Zhou *et al.* correction. The dot-dashed line is a sketch of the nematic-smectic transition boundary.

Let us consider a chain fluid at very low densities, where the virial expansion, when truncated at B_3, provides a good description for the EOS of the system. At these densities p can be approximated as:

$$\frac{p}{kT} = \rho + B_2\rho^2 + B_3\rho^3. \tag{21}$$

By solving the condition of critical point (*i.e.* by setting the first and second derivative of pressure with respect to volume to zero) one obtains:

$$\rho_c - \sqrt{\frac{1}{3B_3}} = 0 \tag{22}$$

$$B_2(T_c) + \sqrt{3B_3(T_c)} = 0. \tag{23}$$

The virial coefficients of a chain of m monomers units from Wertheim's TPT1 theory are given by:[52]

$$B_i = m^i\left[b_i^{\mathrm{ref}} - \frac{m-1}{m}a_i^{\mathrm{ref}}\right] \tag{24}$$

where b_i^{ref} stands for the ith virial coefficient of the monomer reference fluid. Notice that for large values of m the virial coefficient of the chain is given by a power of m times a function of T. The function a_i^{ref} is defined as:

$$\frac{\partial \ln g^{\mathrm{ref}}(\sigma)}{\partial \rho^{\mathrm{ref}}} = a_2 + a_3\rho^{\mathrm{ref}} + \ldots \tag{25}$$

where a_i is the $i-1$ coefficient of the expansion of $\partial \ln(g^{\mathrm{ref}}(\sigma))/\partial\rho^{\mathrm{ref}}$ in powers of the monomer density ρ^{ref}. The relevant feature of eqn. (24) is that the ith virial coefficient of the chain fluid scales as m^i. In fact, one may regard eqn. (23) as an equation defining the value of the critical temperature and eqn. (22) as defining the critical density. For large values of m B_2 scales as m^2 and B_3 scales as m^3. Therefore the first term in eqn. (23) scales as m^2 and the second term as $m^{1.5}$. For large values of m the first term dominates eqn. (23), and therefore eqn. (23) is satisfied only when $B_2(T_c) = 0$. Let us define the critical temperature of the infinitely long chain as the Θ temperature. The Boyle temperature T_B is defined as the temperature at which the second virial coefficient becomes zero. It follows from eqn. (23) that in the limit of large values of m the Θ temperature is just the Boyle temperature of the infinitely long chain. Thus for infinitely long chains we have:

$$\Theta = T_B \tag{26}$$

Moreover for large values of m the result of eqn. (22) is simply $\rho_c = 0$. It is simple to show that $p_c = 0$. By replacing in the virial expansion for Z, the critical density obtained from eqn. (22) and using eqn. (23) it can be shown that for very large values of m the compressibility[53] factor tends to 1/3. Therefore, if the virial expansion truncated in B_3 is sufficient to describe a chain fluid, and if Wertheim's TPT1 is valid to describe the virial coefficients of the chain fluid, then it follows that for very long chains (*i.e.* as m tends to infinity) that the critical number density of chains and the critical pressure go to zero, the compressibility factor goes to 1/3, and that the critical temperature is the Boyle temperature of the infinitely long chain. If higher virial coefficients are included then we have:[52]

$$\Theta = T_B^{\infty} \tag{27}$$

$$T_c(m) = \Theta + \frac{c}{m^{1/2}} + \frac{d}{m} + \ldots \tag{28}$$

$$\rho_c(m) = m^{-3/2} + \ldots \tag{29}$$

$$p_c(m) = m^{-3/2} + \ldots \tag{30}$$

$$Z_c(m) = \frac{1}{3} + \frac{e}{m^2} + \frac{f}{m^3} + \ldots \tag{31}$$

The scaling laws presented by eqns. (28) and (29) are identical to the scaling laws of the Flory–Huggins theory for polymer solutions.[54] The scaling laws for p_c and Z_c are new since the Flory–Huggins theory makes no predictions for the critical pressure or compressibility factor (*i.e.* it is a lattice theory). The variable ρ_c stands for the critical number density of chains. If one is interested in the critical mass density (*i.e.* mass per unit of volume at the critical point) then one must realize that the critical mass density is obtained as the product of the molecular weight that scales as m times the critical number density, which scales as $m^{-1.5}$. Therefore the critical mass density also goes at zero with $m^{-0.5}$. In a sense the previous analysis is an extension of the Flory–Huggins lattice theory to a model in the continuum. Such an extension is made by Wertheim's TPT1 theory. The results presented above[52,53,55] have also been derived independently by Lue *et al.*[56] The fact that according to Wertheim's theory the critical mass density and critical pressure must go to zero for very long chains has important implications. It shows that the critical pressure and mass density of polyethylene must go to zero for very long chains.[53,57,58] In spite of that a number of engineering correlations still propose a non-zero critical pressure, and critical mass density for polyethylene in the limit of infinite molecular weight.[59–61]

The fact that according to Wertheim's TPT1 the Θ temperature must be identical to the Boyle temperature for large values of m has other interesting implications. It follows from eqn. (24) that in the limit of large m the second virial coefficient vanishes when:

$$b_2^{\mathrm{ref}}(\Theta) - a_2^{\mathrm{ref}}(\Theta) = 0. \tag{32}$$

Notice that in the previous equations all terms are related to properties of the reference fluid. By analyzing the virial expansion of $\partial \ln(g^{\mathrm{ref}}(\sigma))/\partial\rho^{\mathrm{ref}}$ in can be shown that the coefficient a_2 is given by:

$$a_2 = 4b_2^{\mathrm{ref}} - 2b_2^{\mathrm{md}} \tag{33}$$

where b_2^{md} is the second virial coefficient between a monomer and a dimer (the dimer being a diatomic molecule formed by two rigidly bonded monomers at a distance σ). By replacing this result in eqn. (32) one obtains:

$$b_2^{\mathrm{ref}}(\Theta) - \frac{2}{3}b_2^{\mathrm{md}}(\Theta) = 0. \tag{34}$$

Eqn. (34) is amazingly simple. It states that according to Wertheim's TPT1 the critical temperature of the infinitely long chain (*i.e.* the Θ temperature) is the temperature where the second virial coefficient of the monomer reference fluid becomes 2/3 of the second virial coefficient between a monomer and a dimer.

Let us now consider the case of a square well chain, with monomers interacting *via* the square well (SW) potential given by:

$$u_0(r) = \begin{cases} \infty = r < d \\ -\varepsilon = d \le r < \lambda d \\ 0 = r \ge \lambda d \end{cases} \tag{35}$$

In this case the second virial coefficient between monomers, b_2^{ref} and the second virial coefficient between a monomer and a dimer b_2^{md} can be computed analytically. Substituting these into eqn. (34) we obtain the Θ temperature for SW chains:

$$\frac{\varepsilon}{k_B\Theta} = \ln\left(\frac{3v_2 - 2V_2 + \sqrt{(2V_2 - 3v_2)^2 + 8V_3(2V_T - 3v_T)}}{4V_3}\right) \tag{36}$$

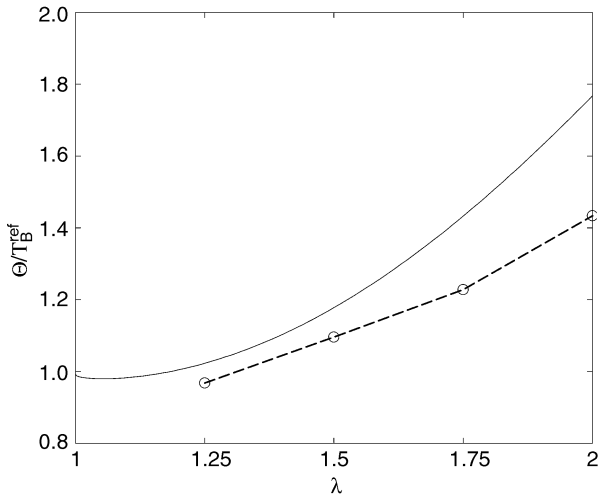

Fig. 18 Ratio between Θ and the Boyle temperature of the reference fluid T_B^{ref} for SW chains as obtained from TPT1 (solid line) or from the numerical results of Hall *et al.* (symbols).

where v_2, V_2, V_3, V_T, v_T are analytical functions of λ (see ref. 55 for details). This a simple and interesting result. It means that the Θ temperatures that follow from Wertheim's TPT1 can be calculated with a pocket calculator. Eqn. (36) gives the value of the Θ temperature of SW chains (obtained from Wertheim's TPT1 theory) as a function of λ. In Fig. 18 the Θ temperature of SW chains is plotted as a function of the range of the potential λ. Instead of plotting Θ, the ratio of Θ to the Boyle temperature of the monomer fluid (denoted as T_B^{ref}) has been plotted. The solid line are the results from Wertheims's TPT1 theory (see eqn. (36)) whereas the dashed line correspond to the estimate of the Boyle temperature of infinitely long SW chains obtained numerically by Hall *et al.*[62,63]

Some interesting features present in Fig. 18 are the following:

(i) The ratio Θ/T_B^{ref} is of order unity. In other words the Θ temperature of SW chains is close to the Boyle temperature of the monomer reference fluid.

(ii) In general the ratio Θ/T_B^{ref} increases as λ increases.

(iii) Wertheim's TPT1 overestimates the Θ temperature of the polymer by 15%. Notice that in our description of the reference fluid b_2^{ref} is determined analytically so that T_B^{ref} is obtained exactly. The discrepancy between theory and simulation observed in Fig. 18 is exclusively due to the inaccuracy of the theory in determining Θ. Other authors have also noticed that Wertheim's TPT1 overestimates the critical temperature of SW chains for finite values of m.[49] Here we show that the same is true for the critical temperature of infinitely long chains.

VI. Conclusions

In this work the effect on flexibility on the phase diagram has been studied for a number of simple models. The focus has mainly been on hard models. Three models were considered representing extreme cases. The first corresponds to a fully flexible chain, the second to a rigid linear chain, and the third to a hybrid model with rigid and flexible parts. For each of these models, virial coefficient calculations, and NpT Monte Carlo simulations were performed in order to determine the differences and similarities in their behavior. For all phases with an isotropic distribution of bond vectors we implement Wertheim's TPT1 theory (*i.e.* all isotropic fluid phases and the solid phase of the pearl-necklace model). From this study we can draw the following conclusions:

(i) Virial coefficients of rigid and flexible chains differ considerably in their values and in their scaling laws. However the value of B_3 seems to be quite similar for both models (at least for the values of m) considered.

(ii) At medium densities the EOS does not depend on the presence or absence of flexibility. Wertheim's TPT1 for the EOS performs well in this density range. Although the individual virial coefficients of rigid and flexible chains differ considerably, it seems that their sum is insensitive to the presence or absence of flexibility.

(iii) The phase diagram of the pearl-necklace model is somewhat unsurprising: displaying an isotropic fluid phase and an ordered solid with disordered bonds. This was shown previously by Malanoski and Monson. We have demonstrated that Wertheim's TPT1 can be implemented to describe the freezing properties of this model with high accuracy. In fact Wertheim's TPT1 predicts that the freezing properties of the pearl-necklace model tend to asymptotic finite values for large values of m. For instance the volume fraction at freezing for flexible chains tends to 0.54 (hard spheres monomers freezes at a volume fraction of about 0.49). Moreover the p^* *versus* y plot is almost independent of m for $m > 6$.

(iv) The phase behavior of rigid chains is more complex than for flexible chains. For $m = 6$, isotropic, nematic, smectic A and solid phases were found. The volume fraction at which the isotropic–nematic transition occurs moves to zero as m increases. However the volume fractions for the nematic–smectic A, and smectic A–solid transitions is hardly affected by m. For a given volume fraction the reduced pressure of the fully rigid model is always below that of the flexible model. This is mostly due to the appearance of phases where the molecular bonds are ordered. This is the case of the solid, smectic A and nematic phases. When the distribution of bond vectors is isotropic, differences suddenly disappear between rigid and flexible chain models.

(v) For the hybrid model (both rigid and flexible sections) we found that the more flexible the molecule is the narrower is the region of liquid crystal behavior and the later its onset. Moreover it is found that flexibility destabilizes the nematic phases and promotes the smectic phase.

(vi) For systems with LJ monomer beads our understanding of the phase diagram is far from complete. A full comparison between rigid and flexible molecules for these kind of molecules would be very interesting. Here we have focused on the vapor–liquid equilibria of flexible chains as obtained from Wertheim's TPT1. We have shown that according to Wertheim's TPT1 the number density, mass density and pressure vanishes at the critical point for infinitely long chains. The compressibility factor however tends to a finite non-zero value. The same is true for the critical temperature which tends to the Boyle temperature of the infinitely long chain. Essentially we recover the original results from the Flory–Huggins lattice theory but now based on a well defined non-lattice fluid theory. The Boyle temperature of this infinitely long chain that follows from Wertheim's TPT1 can be obtained by solving a simple equation where only the second virial coefficient of the monomer and the second virial coefficient between a monomer and a dimer appears. In the particular case of square well chains, these virial coefficients can be computed analytically, thus yielding a simple analytical equation for the Θ temperature of square well chains. The Θ temperature is of the order of the Boyle temperature of the monomer, and for reasonable values for the range of the potential, somewhat larger.

In our view a number of problems remain to be clarified. In particular the extension of Wertheim's theory to phases with ordered bonds would be an important step. Also the determination of the phase diagram of LJ flexible chains would be quite useful. The same is true for the LJ version of the rigid linear chains. Certainly the fully flexible model is somewhat

unrealistic and this is reflected in the "curious" type of solid phase that it adopts. However, notice that by imposing an arbitrary fixed bond angle (even in a model with tangent flexible spheres) the existence of a fcc close packed structure for the atoms becomes impossible. In this case the system must freeze into a solid with ordering of bonds and with a substantial decrease in the flexibility of the molecule in the solid phase. The study of such a model would bring us closer to a polymer system.

Acknowledgements

Financial support is due to project No. BFM2001-01420-C02-01 of the Spanish DGICYT (Dirección General de Investigación Científica y Técnica). One of the authors, C. M., would like to acknowledge and thank the European Union EP5 Program for the award of a Marie Curie post-doctoral fellowship (N°, HPMF-CT-1999-00163). We also wish to thank the "Centro de Supercomputacion" of Universidad Complutense de Madrid for a generous allocation of computer time on their SGI Origin 2000.

References

1 C. G. Gray and K. E. Gubbins, *Theory of molecular fluids*, Clarendon Press, Oxford, 1984.
2 P. J. Flory, *Statistical Mechanics of Chain Molecules*, Hanser Publishers, Munich, 1969.
3 S. J. Clark, C. J. Adam, D. J. Cleaver and J. Crain, *Liq. Cryst.*, 1997, **22**, 477.
4 S. J. Clark, G. J. Ackland and J. Crain, *Europhys. Lett.*, 1998, **44**, 578.
5 M. P. Allen and D. J. Tildesley, *Computer simulation of liquids*, Oxford University Press, Oxford, 1987, ch. 1.
6 K. G. Honnell and C. K. Hall, *J. Chem. Phys.*, 1989, **90**, 1841.
7 A. Yethiraj, C. K. Hall and K. G. Honnell, *J. Chem. Phys.*, 1990, **93**, 4453.
8 R. Dickman and C. K. Hall, *J. Chem. Phys.*, 1988, **89**, 3168.
9 C. McBride, C. Vega and L. MacDowell, *Phys. Rev. E*, 2001, **64**, 011703.
10 M. S. Wertheim, *J. Chem. Phys.*, 1987, **87**, 7323.
11 M. S. Wertheim, *J. Stat. Phys.*, 1984, **35**, 19.
12 M. S. Wertheim, *J. Stat. Phys.*, 1984, **35**, 35.
13 M. S. Wertheim, *J. Stat. Phys.*, 1986, **42**, 459.
14 M. S. Wertheim, *J. Stat. Phys.*, 1986, **42**, 477.
15 W. G. Chapman, G. Jackson and K. E. Gubbins, *Mol. Phys.*, 1988, **65**, 1.
16 T. Boublik, C. Vega and M. D. Pena, *J. Chem. Phys.*, 1990, **93**, 730.
17 Y. Zhou and G. Stell, *J. Chem. Phys.*, 1992, **96**, 1507.
18 J. K. Johnson, J. A. Zollweg and K. E. Gubbins, *Mol. Phys.*, 1993, **78**, 591.
19 J. K. Johnson, E. A. Muller and K. E. Gubbins, *J. Phys. Chem.*, 1994, **98**, 6413.
20 R. J. Sadus, *Mol. Phys.*, 1999, **97**, 1279.
21 N. F. Carnahan and K. E. Starling, *J. Chem. Phys.*, 1969, **51**, 635.
22 Y. Song, S. M. Lambert and J. M. Prausnitz, *Macromolecules*, 1994, **27**, 441.
23 Y. C. Chiew, *Mol. Phys.*, 1990, **70**, 129.
24 F. H. Ree and W. G. Hoover, *J. Chem. Phys.*, 1964, **40**, 939.
25 M. Rigby, *Mol. Phys.*, 1989, **66**, 1261.
26 M. Rigby, *J. Chem. Phys.*, 1970, **53**, 1021.
27 C. Vega, *Mol. Phys.*, 2000, **98**, 973.
28 C. Vega, S. Lago and B. Garzon, *Mol. Phys.*, 1994, **83**, 1233.
29 C. Vega, J. M. Labaig, L. G. MacDowell and E. Sanz, *J. Chem. Phys.*, 2000, **113**, 10398.
30 A. Yethiraj, K. G. Honnell and C. K. Hall, *Macromolecules*, 1992, **25**, 3979.
31 D. C. Williamson and G. Jackson, *Mol. Phys.*, 1995, **86**, 819.
32 K. M. Jaffer, S. B. Opps and D. E. Sullivan, *J. Chem. Phys.*, 1999, **110**, 11630.
33 P. G. de Gennes, *Scaling concepts in polymer physics*, Cornell University Press, Ithaca, 1979.
34 L. Onsager, *Ann. NY Acad. Sci.*, 1949, **51**, 627.
35 D. Frenkel, *J. Phys. Chem.*, 1988, **92**, 5314.
36 D. Frenkel, *J. Phys. Chem.*, 1987, **91**, 4912.
37 D. Frenkel, *J. Phys. Chem.*, 1988, **92**, 3280.
38 A. P. Malanoski and P. A. Monson, *J. Chem. Phys.*, 1997, **107**, 6899.
39 K. W. Wojciechowski, D. Frenkel and A. C. Brańka, *Phys. Rev. Lett.*, 1991, **66**, 3168.
40 C. Vega and L. MacDowell, *J. Chem. Phys.*, 2001, **114**, 10411.
41 C. Vega, E. P. A. Paras and P. A. Monson, *J. Chem. Phys.*, 1992, **96**, 9060.
42 S. Yashonath and C. N. R. Rao, *Mol. Phys.*, 1985, **54**, 245.
43 C. Vega, C. McBride and L. MacDowell, *J. Chem. Phys.*, 2001, **115**, 4203.
44 C. Vega and S. Lago, *J. Chem. Phys.*, 1994, **100**, 6727.
45 D. C. Williamson and G. Jackson, *J. Chem. Phys.*, 1998, **108**, 10294.
46 P. Bolhuis and D. Frenkel, *J. Chem. Phys.*, 1997, **106**, 666.
47 D. Frenkel and B. Smit, *Understanding Molecular Simulation*, Academic Press, San Diego, 1996.
48 Y. Zhou, C. K. Hall and G. Stell, *J. Chem. Phys.*, 1995, **103**, 2688.
49 F. A. Escobedo and J. J. D. Pablo, *Mol. Phys.*, 1996, **87**, 347.
50 F. J. Blas and L. F. Vega, *Mol. Phys.*, 1997, **92**, 1.
51 Y. J. Sheng, A. Z. Panagiotopoulos and S. K. Kumar, *Macromolecules*, 1994, **27**, 400.
52 L. G. MacDowell, M. Muller, C. Vega and K. Binder, *J. Chem. Phys.*, 2000, **113**, 419.
53 C. Vega and L.G. MacDowell, *Mol. Phys.*, 1996, **88**, 1575.
54 P. J. Flory, *Principles of polymer chemistry*, Cornell University Press, Ithaca, 1954.
55 C. Vega and L. G. MacDowell, *Mol. Phys.*, 2000, **98**, 1295.
56 L. Lue, D. G. Friend and J. R. E. Elliot Jr., *Mol. Phys.*, 2000, **98**, 1473.
57 E. D. Nitikin, *High Temp.*, 1998, **36**, 322.
58 L. G. MacDowell and C. Vega, *J. Chem. Phys.*, 1998, **109**, 5681.
59 C. Tsonopoulos and Z. Tan, *Fluid Phase Equilib.*, 1993, **83**, 127.
60 H. Korsten, *Chem. Eng. Technol.*, 1998, **21**, 229.
61 T. T. M. Tan and B. M. Rode, *Macromol. Theory Simul.*, 1995, **4**, 983.
62 J. Dautenhahn and C. K. Hall, *Macromolecules*, 1994, **27**, 5399.
63 J. M. Wichert and C. K. Hall, *Macromolecules*, 1994, **27**, 2744.